

# We are IntechOpen, the world's leading publisher of Open Access books Built by scientists, for scientists

6,900

Open access books available

186,000

International authors and editors

200M

Downloads

Our authors are among the

154

Countries delivered to

TOP 1%

most cited scientists

12.2%

Contributors from top 500 universities



WEB OF SCIENCE™

Selection of our books indexed in the Book Citation Index  
in Web of Science™ Core Collection (BKCI)

Interested in publishing with us?  
Contact [book.department@intechopen.com](mailto:book.department@intechopen.com)

Numbers displayed above are based on latest data collected.  
For more information visit [www.intechopen.com](http://www.intechopen.com)



# Doping of Polymers with ZnO Nanostructures for Optoelectronic and Sensor Applications

Aga and Mu  
Fisk University  
USA

## 1. Introduction

The discovery of new materials with unique properties often leads to new technology. After discovery of conductive polymers at the end of the 1970s, it opened up a whole new research, which eventually led to a new technology of plastic electronics (Chiang et al., 1978). When interesting material properties are observed in the laboratory, efforts are made to understand their mechanisms, which leads to the fine control of the fabrication process of this new and potentially important material. If future applications are anticipated, optimization of material properties becomes a continuous and sometimes a lifelong process. Doping of materials is one of the ways of modifying their physical properties. For example, a pure silicon (Si), which has a very poor electrical conducting properties can be doped with boron or arsenic to make it a good hole or electron conductor respectively. This opened up a new class of doped-Si materials, which is now the basis of perhaps the largest global electronics industry.

Polymers, which consist of large molecules linked together in repeated fashion to form long chains, have naturally existed for a long time. Examples are tortoise shell, tar and horns. Today synthetic polymers are finding important applications in many areas. Polyolefins, epoxies and engineering resins are crucial materials for construction, commerce, transportation and entertainment. They are very appealing alternative materials because of the simple processing they offer such as drop casting, spray painting and printing. In addition, they almost provide low cost large-area scalability. In most applications however, polymeric materials are multicomponent systems. The integration of fillers such as minerals, ceramics, metals or even air, can generate an infinite variety of new materials with unique physical properties and possibly reduced production cost. Typically, when the filler in these multicomponent systems, which represents a minor constituent, has at least one dimension below 100 nm, the resulting material is termed, "polymer nanocomposite" (Winey & Vaia, 2007). Research in this area is very active and promising, mainly because of many different combinations of polymers and filler materials that can be explored. Few examples of fillers that were recently reported are SrTiO<sub>3</sub> (Umeda et al., 2009), fluorinated single walled carbon nanotubes (Bennett et al., 2009) and ZnS-coated CdSe nanocrystals (Kim et al., 2009).

The addition of a small amount of filler material into a host polymer can be considered a doping process if there is an intention of modifying the physical properties of the host. Some fillers, particularly with macroscopic dimensions, do not chemically react with the polymer so they cannot be regarded as dopants. Nanomaterials are attractive dopants to polymers

Source: Nanowires Science and Technology, Book edited by: Nicoleta Lupu,  
ISBN 978-953-7619-89-3, pp. 402, February 2010, INTECH, Croatia, downloaded from SCIYO.COM

because of their high surface reactivity, which is attributed to very large surface-to-volume ratio. Moreover, they possess intriguing properties associated with quantum confinement effects, making their interaction with different polymers a subject of great interest. They can also be dispersed into water or organic solvents, providing a simple process of doping polymeric solutions. It should be realized that nanomaterial-doped polymers should also be classified as polymer nanocomposite because they are multicomponents systems with a low dimensional non-polymer minor constituent embedded in a host polymer. When the nanomaterial dopant is inorganic, the term “hybrid nanocomposite” is specifically used for the reason that it becomes an inorganic-organic system. This manuscript focuses on the effect of doping polymers with ZnO nanostructures such as nanowires, nanorods, tetrapods and nanoparticles. Their combination may achieve three goals: 1) tailor the property of ZnO; 2) tailor the property of polymer or 3) create a hybrid nanocomposite with unique or enhanced properties. A discussion of how these goals are relevant for optoelectronic and sensor applications is presented.

## 2. ZnO as dopant to polymers

### 2.1 Technological importance of ZnO

ZnO has received much attention in recent years due to its diverse properties. It is a direct wide bandgap semiconductor ( $E_g = 3.4$  eV) with large exciton binding energy ( $\sim 60$  meV), suggesting that it is a promising candidate for stable room temperature luminescent and lasing devices. It exhibits strong ultraviolet (Huang et al., 2001) and visible photoluminescence (Konenkamp et al., 2004). ZnO film can be used as transparent conducting electrode. It is also a piezoelectric material, with potential applications in surface acoustic wave filters (Wang et al., 2008). Ferromagnetism in ZnO has already been reported (Kim et al., 2009) so it is being considered a material for spintronics. With all these important properties, it becomes more attractive because of its abundance in nature. It can be fabricated practically into different forms like thin film and nanowire using a variety of methods such as solution-based approaches, vacuum deposition techniques chemical vapor deposition.

### 2.2 Fabrication of ZnO nanostructures for dispersion in solution

There are several ways of fabricating ZnO nanostructures on a substrate. Nanowires, nanorods, nanobelts, nanoneedles and nanosprings have been reported by many researchers. For doping polymers, it is advantageous for the nanostructures to be dispersed in a solution since most polymers are prepared via a solution process. ZnO nanostructures grown on a substrate can be scraped and dispersed into a solvent. This approach however does not produce enough amount of nanostructures. Hence, it is not a practical method for obtaining a usable concentration of ZnO in a solvent. Solution-based methods have been widely used to prepare ZnO nanostructures. Nanorods and nanowires with variable-aspect-ratio (length/diameter) have been prepared in alcohol/water solution by reacting a  $Zn^{2+}$  precursor with an organic weak base, tetramethylammonium hydroxide ( $Me_4NOH$ ) at temperature window of  $75 - 150$  °C (Cheng et al., 2006). In another report, a room temperature wet-chemical approach was employed to synthesize highly regulated, monodispersed ZnO nanorods and derived hierarchical nanostructures such as hexagonally branched, reversed umbrella-type and cactus-like (Liu & Zeng, 2004). These hierarchical nanostructures are comprised of individual *c*-oriented nanorods. In the typical synthesis, the

precursor solution of Zn was prepared by dissolving zinc nitrate and sodium hydroxide in deionized water. A sample of pure ethanol was added followed by ethylenediamine. The mixed solution was covered and kept at room temperature under constant stirring for 1-12 days to form the ZnO nanorods. ZnO nanoparticles with size ranging from 2 to 7 nm can also be prepared by addition of lithium hydroxide to an ethanolic zinc acetate solution (Meulenkamp, 1998).

One of the disadvantages of solution-based ZnO fabrication is that it involves successive processes that take a fair amount of time. After the synthesis, the product has to be thoroughly cleaned to remove all traces of chemicals used in the process. In this article, a simple, straightforward method to fabricate ZnO nanostructures with fast turn around is explored. It is based on the oxidation of zinc vapor while a high purity Zn metal is being thermally evaporated. Figure 1 is a diagram that illustrates this method. The Zn source is placed in a crucible, which is then inserted into a vertically-oriented quartz tube. The tube is flushed with argon to remove ambient air and its open end is sealed [Figure 1(a)]. It is inserted into a vertically-oriented furnace set at 600 °C to evaporate the Zn. When the source starts to evaporate, air is allowed to diffuse towards the crucible by opening the seal. With the correct diffusion rate of O<sub>2</sub> and evaporation rate of Zn, oxidation can be contained inside the crucible. Thus, the growth of ZnO nanostructures mainly occurs in the crucible. Figure 1(b) shows the actual crucible before and after the growth process. Typically, when the amount of Zn source is 0.03 g, it yields approximately 0.01 g of ZnO, which is the white material that fills the crucible in the picture. The product is like a cotton as shown by the SEM picture in Figure 1(c). It can be easily collected and dispersed in a solution. The entire fabrication process only takes less than 30 minutes. It is highly scalable and can be employed to mass-produce ZnO nanostructures.

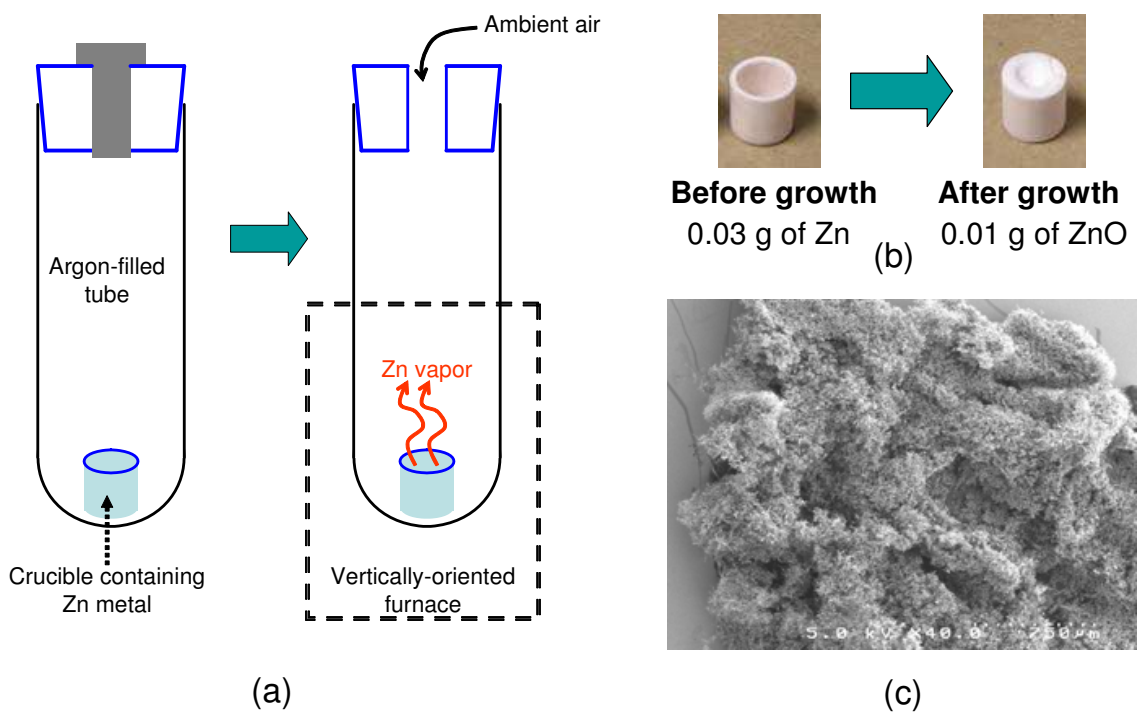


Fig. 1. (a) Diagram illustrating the simple fabrication process of ZnO nanostructures. (b) Photos of the actual crucible before and after the growth process. (c) SEM picture of the cotton-like ZnO product collected from the crucible.

The cotton-like ZnO product shown in Figure 1(c) consists of different nanostructures entangled together. They can be separated and size selected if desired. Two solvents were tried to disperse them: water and chlorobenzene. By ultrasonication, they were effectively segregated in both solvents. The solution became whitish after several minutes of agitation. When the procedure was stopped, ZnO structures slowly settled at the bottom and as expected, large entities sank first. This can be used as a simple size-selection method. For example, nanoparticles with lower diameter are the last ones to settle at the bottom. If the solution is allowed to be still for a long time after sonication, then get the top part of it, nanoparticles are obtained. They are shown in Figure 2(a). They are deposited on Si wafer by drop casting. If the large and unwanted entities are already removed, good nanowires can be extracted from the bottom of the solution. These nanowires are shown in Figure 2(b). Their length could exceed 10  $\mu\text{m}$ .

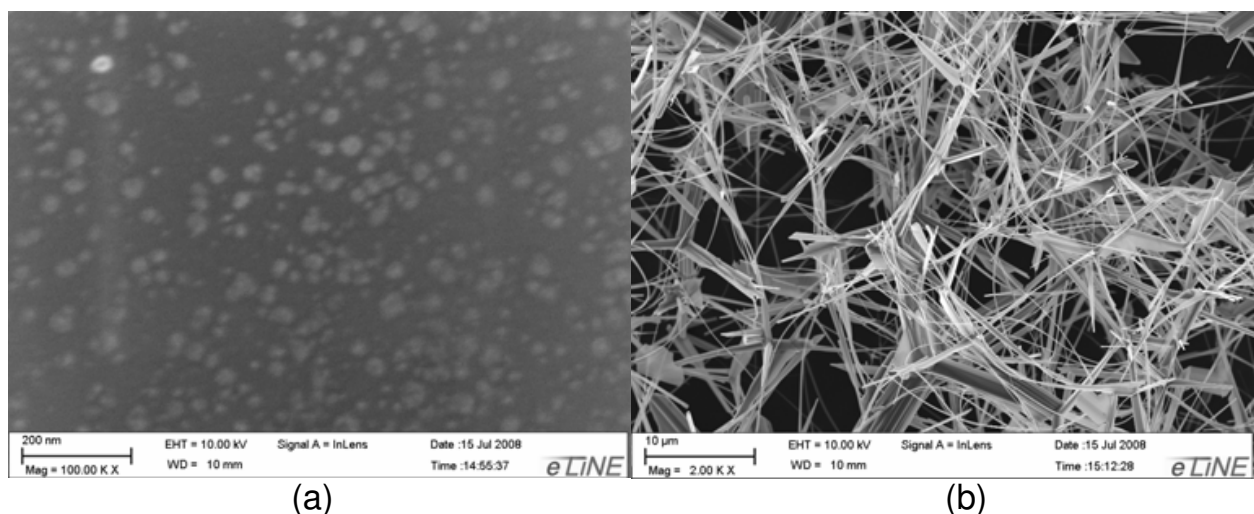


Fig. 2. SEM micrographs of (a) ZnO nanoparticles and (b) ZnO nanowires via a mass production method and deposited on Si wafer after a simple size-selection process.

### 3. Polymer-based light emitting devices

#### 3.1 Basic requirements for efficient electroluminescence

Polymeric-based light emitting device is one type of OLED, which stands for organic light emitting diode. Photon is generated in the polymer emissive layer (EL), which should possess excellent photoluminescence (PL) properties. In an efficient device, the EL is sandwiched between an electron transport layer (ETL), which injects electrons into the LUMO (lowest unoccupied molecular orbital) of the EL, and a hole transport layer (HTL), which injects holes into the HOMO (highest occupied molecular orbital) of the EL. The injected electrons and holes undergo radiative recombination due to the applied electric field. The charge transporting layers serve as facilitator for efficient charge transfer from the electrodes to the EL. This is illustrated in Figure 3. When a negative potential is applied to the anode, which is a low work function metal, electrons are injected into the ETL. If the ETL has excellent electron mobility (*n*-type) and its LUMO aligns closely with the LUMO of EL and the work function of the anode, efficient electron charge transport towards the EL is achieved. On the other hand, the positive potential applied to the cathode, which is a high work function transparent conductor, results in the injection of holes into the HTL. Efficient

hole transport towards the EL is achieved if the HTL has excellent hole mobility ( $p$ -type) and its HOMO is well aligned with the HOMO of the EL and the work function of the cathode. It should be realized that the realization of high efficient OLEDs depends not only on the electronic and optical properties of the EL material, but also on the control of charge transport in the device.

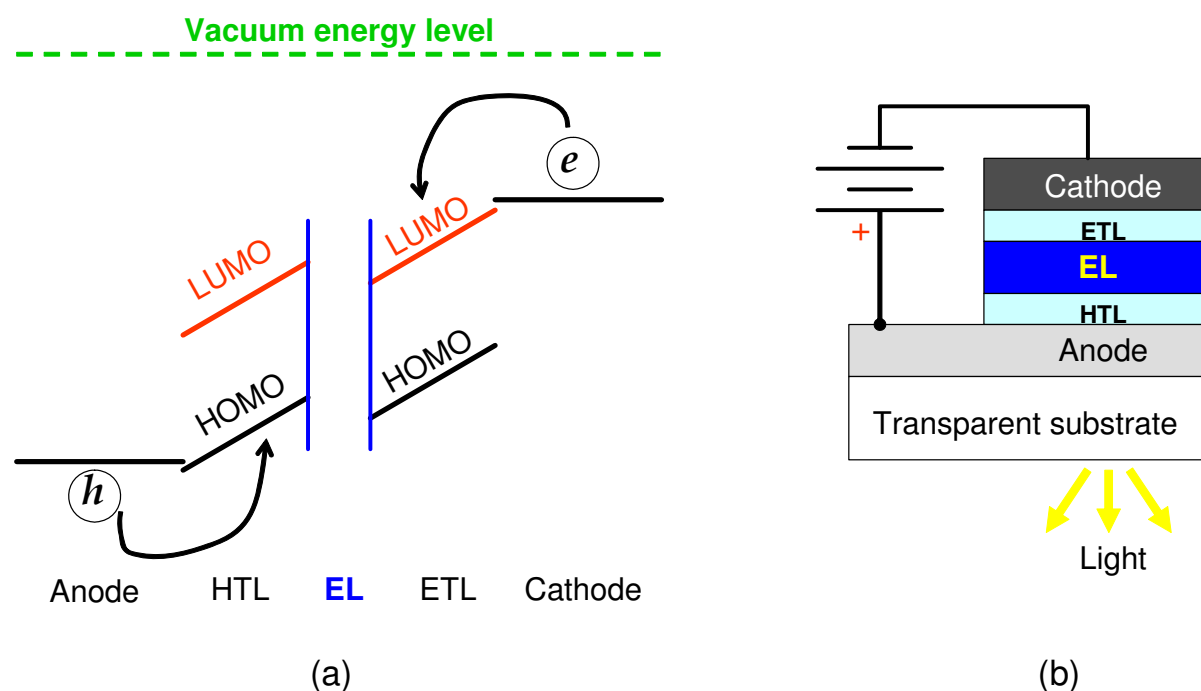


Fig. 3. (a) Operation of a polymeric OLED and its (b) device structure.

### 3.2 Control of charge transport

One of the benefits of doping polymers in OLED with ZnO nanostructures is the improvement in charge carrier transport. It has been reported that by incorporating ZnO nanorods with the EL material PVK:DCJTb, which represents poly(vinylcarbazole) doped with 4-(dicyanomethylene)-2-*t*-butyl-6-(1,1,7,7-tetramethyljulolidyl-9-enyl)-4H-pyran at 1%, low threshold voltage and higher electroluminescence efficiency is obtained (Zhang et al., 2006). The authors employed the device structure: ITO/EL/Alq<sub>3</sub>/Al, with different concentrations of ZnO (1 wt%, 5 wt%, 10 wt%) in the EL material. They observed that the hole current density increases with increasing concentration of ZnO nanorods. This made the current injection more balanced and consequently enhanced the electroluminescence efficiency. They explained the increase in the hole current in terms of the effect of ZnO on the molecular chain of PVK. The nanorods can make the PVK chain more unwindable and possibly connect aligned molecular chains. Thus, current is not limited by hopping of carriers between chains. In addition, wurtzite ZnO has higher hole mobility ( $\mu_h$ ) than PVK. For low  $p$ -type conductivity at room temperature, it ranges from 5 to 50 cm<sup>2</sup>/V-s (Norton et al., 2004). For PVK at low electric fields, it is in the order of 10<sup>-7</sup> cm<sup>2</sup>/V-s (Blom et al., 1997). A similar observation has been reported on poly[2-methoxy,5-(2-ethylhexyloxy)-1,4-phenylenevinylene], which is commonly called MEH-PPV for short (Xu et al., 2007). By doping the MEH-PPV with ZnO nanocrystals or tetrapods and employing it to build field effect transistor, the authors showed higher  $p$ -type mobility in the polymer nanocomposite.

Pure MEH-PPV, which only exhibits *p* - channel behaviour, has  $\mu_h$  value in the order of  $10^{-4}$   $\text{cm}^2/\text{V}\cdot\text{s}$ . This increases with increasing concentration of ZnO nanostructures and saturates at 40 wt%. For nanocrystals and tetrapods,  $\mu_h$  saturates at a value of about  $0.08 \text{ cm}^2/\text{V}\cdot\text{s}$  and  $0.15 \text{ cm}^2/\text{V}\cdot\text{s}$  respectively. It should be mentioned that doping with ZnO did not change the conductivity type, indicating that charge transport takes place in the polymer. This is not surprising because there is a large energy barrier for holes to be transferred from ZnO to MEH-PPV. The valence band edge for ZnO is 7.6 eV while the HOMO of MEH-PPV is 5.3 eV. When the density of traps was investigated, it was found that it decreases with increasing ZnO concentration. Interestingly, it also saturates at 40 wt%. This is a strong indication that the effect of ZnO is to reduce the density of traps in the polymer and consequently improve its  $\mu_h$ . The authors further supported this interpretation by transient current measurement where a constant bias voltage was applied to the gate and the drain. The decrease in channel current with time was more dramatic for the pure polymer than the nanocomposite. This suggests that charge trapping is significantly reduced by ZnO doping. Other authors propose that the enhancement in  $\mu_h$  is due to the superposition of several transport mechanisms in the nanocomposite including percolation through polymer-ZnO nanoparticle interface network (Aleshin et al., 2008).

### 3.3 Control of optical emission

The high surface reactivity of ZnO nanostructures with certain polymers may provide interactions that can modify polymer properties in a positive way. The interaction of ZnO quantum dots (QDs) with poly(vinyl alcohol) (PVA) has already been demonstrated (Sui et al., 2005). The authors prepared PVA/ZnO hybrid nanofibers with ZnO concentration of 10 wt% and employed differential scanning calorimetry (DSC) to study them with respect to pure PVA. It is known that the two exothermic peaks at about 305 °C and 500 °C are associated with the degradation of side chain (the scission of C-O) and main chain (the scission of C-C) with the delta enthalpy of 3760 and 1188  $\text{J g}^{-1}$ , respectively (Koji et al., 1999). For PVA/ZnO nanofibers, the exothermic peak below 450 °C was not observed, while the peak around 500 °C was sharp and strong with delta enthalpy of 3305  $\text{J g}^{-1}$ , suggesting that ZnO modifies the property of PVA. Their interaction, which is via the formation of an H bond and an O-Zn-O bond between PVA molecule and ZnO, is believed to be responsible for the novel luminescent properties of PVA/ZnO nanofibers.

Figure 4 shows a typical PL spectrum of ZnO nanowires (NWs) prepared by the physical vapor transport method described in section 2.2. It has two emission bands around 380 and 520 nm, which is consistent with another report using a polymer-assisted route (Li et al., 2003). The UV emission originates primarily from a mixture of free exciton and bound exciton related to impurity or defects (Shan et al., 2005). The visible emission comes from the transition between the electron near the conduction band and the deeply trapped hole at the  $V_0^{**}$  center which is an oxygen vacancy containing no electrons (Dijken et al., 2000). It is also attributed to the transition between the electron at  $[V_0^*, \text{electron}]$  or  $[V_0^{**}, \text{two electrons}]$  and the hole at vacancy associated with the surface defects. For pure PVA, the PL spectrum consists of two emission bands at about 364 and 440 nm, originating from its organic functional groups (Sui et al., 2005). In PVA/ZnO hybrid film, the PL spectrum is a superposition of the PL of each component. The 440 nm emission from PVA overlaps with the 550 nm from ZnO making the visible emission band broader. In hybrid nanofibers however, this visible emission is much intense possibly due to two factors. In the film, ZnO-

QDs can easily form aggregates resulting in bigger particle exhibiting bulk behavior. This is in fact one of the issues in polymer nanocomposites and ways to circumvent it are being explored (Sun et al., 2008). In the nanofiber, QDs align along the PVA matrix, resulting in better dispersion. Individual QD also interacts strongly with the PVA molecule. The other factor is the high surface to volume ratio of the nanofiber, which enhances the visible luminescence due to surface defects (Shalish et al., 2004).

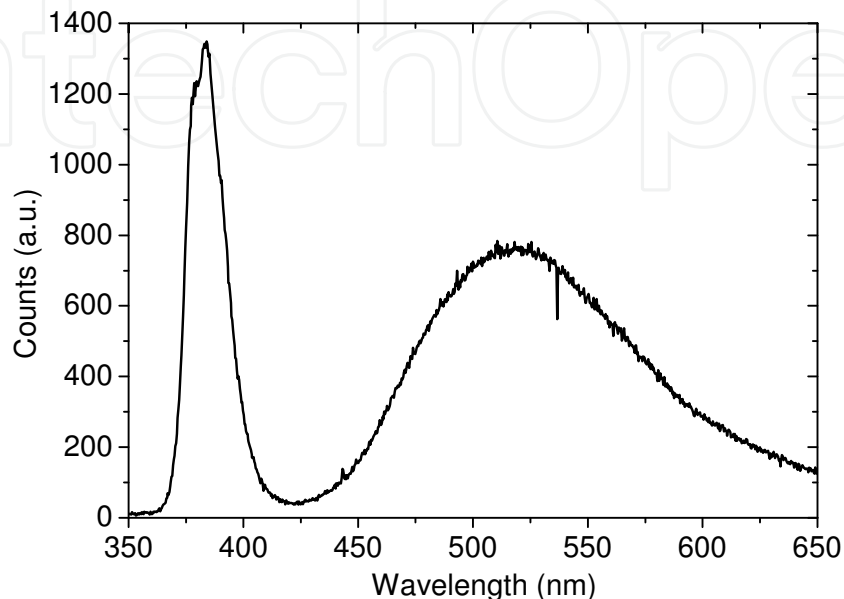


Fig. 4. Photoluminescence (PL) spectrum of ZnO nanowires for polymer doping, grown by physical vapour transport.

The interaction between ZnO and polymer can also provide several new radiative recombination mechanisms that may be utilized for broadband light emission or wavelength tunable emission. Since these mechanisms are influenced by several factors such as the individual properties of the organic and inorganic components as well as their relative concentration, control of emission properties may be done in a number of ways. The existence of new recombination mechanisms is strongly suggested by the generation of new PL emission lines (420, 460 & 480 nm) when MEH-PPV is doped with ZnO nanoparticles (Aleshin et al., 2009). In this work, the authors prepared the polymer nanocomposite film on a Si substrate with a 200 nm-thick SiO<sub>2</sub> layer via drop casting or spin coating. Gold and aluminum electrodes were then deposited on top with separation of 7 - 15  $\mu\text{m}$ . With this device structure, they could investigate PL while applying an external electric field. The existence of new emission lines, which could not be generated when ZnO was replaced by Si nanoparticles, was attributed to the formation of interfacial states termed exciplex. These states are formed in a type II heterojunction, such as ZnO/MEH-PPV, where there is an accumulation of electrons and holes on the opposite side. Charge transport is blocked by the barriers that result from the offset of HOMO and conduction band edge of MEH-PPV and ZnO respectively. It was proposed that since the carriers cannot proceed across the heterojunction, they diffuse two-dimensionally along the interface until they encounter an oppositely charged carrier on the opposite side of the interface and these form an exciplex (Morteani et al., 2005). If bulk exciton in the ZnO or MEH-PPV is within the exciton diffusion length, it can excite exciplex emission. It should be mentioned that the influence of

ZnO nanoparticles is most dramatic at an optimum concentration of 10 wt%. This could be ascribed to the aggregation of nanoparticles which reduces interaction with polymer.

Another observed phenomena when MEH-PPV is doped with ZnO is the blue shift of its PL emission spectrum accompanied by quenching. At 2 wt% concentration of ZnO nanoparticles, 11 nm shift has been reported (Ton-That et al., 2008). This shift increases with increasing nanoparticle concentration. However, its dependence becomes weaker at concentration greater than 4%. Using Raman spectroscopy, the authors did not observe any changes in the conjugation length, which may have caused the blue shift in PL spectrum. Their results indicate that the chemical structure and the gap energy of MEH-PPV is not affected by the incorporation of ZnO nanoparticles. Thus, they explained their observation in terms of the effect of electric field produced by excess electrons on the nanoparticles surface (Musikhin et al., 2002). The surface of ZnO nanoparticles is a strong perturbation of the lattice where there exists a high concentration of both shallow and deep defect levels (Ton-That et al., 2008). X-ray photoelectron spectroscopy (XPS) analysis of their surface revealed that there is a large number of oxygen vacancies. These vacancies can accept electrons from MEH-PPV, creating an electric field outside the nanoparticles. As a result, the energy of the lowest exciton state is raised resulting in the blue shift of the luminescence.

## 4. Polymer-based photovoltaics

### 4.1 Challenges

The highest power conversion efficiency ( $\eta$ ) demonstrated by a polymer-based solar cell is achieved by employing an active layer blend of poly(3-hexylthiophene) and (6,6)-phenyl C61 butyric acid methyl ester (Ma et al., 2005). For convenience, this blend will be referred as P3HT:PCBM. It has a strong optical absorbance in the limited wavelength range of 400 nm to 600 nm mainly due to the P3HT. Because of this narrow band absorption, more than 60% of the photons in the solar spectrum are not harnessed. In fact, even the ones absorbed are not 100% converted to photocurrent because not all electron-hole pairs become free charges. Exciton binding energy of P3HT is so large that it does not lead directly to free charge carriers. However, the high electron affinity of PCBM provides sufficient potential difference that breaks exciton and thus it becomes energetically favourable for the electrons to jump from the LUMO of P3HT to the LUMO of PCBM. This electron donor-acceptor mechanism implies that only excitons near the P3HT/PCBM interface dissociate. The maximum distance for dissociation to occur is determined by the exciton diffusion length ( $\tau$ ), which is around 10 nm for P3HT. In the blend, phase segregation results in the formation of isolated islands of P3HT and PCBM. The size of P3HT islands could be more than  $\tau$  so not all excitons can dissociate. There is another factor in the exciton dissociation process that reduces  $\eta$ . Excited electrons in P3HT have excess energy that is dissipated quickly when they transfer to the PCBM. This energy loss, which depends on the energy alignment of the two materials, is reflected in the open circuit voltage (Koster et al., 2006).

In a photovoltaic device, separated holes and electrons need to reach their respective electrodes to have high  $\eta$ . This requires the blend to have high values of hole ( $\mu_h$ ) and electron ( $\mu_e$ ) mobilities. Good balance of mobilities is obtained using optimum ratio of P3HT and PCBM, which is estimated to be between 1:1 and 1:0.9 (Chirvase et al., 2004). This could yield values of  $\mu_h \sim 6.5 \times 10^{-6} \text{ cm}^2/\text{V-s}$  and  $\mu_e \sim 5.0 \times 10^{-6} \text{ cm}^2/\text{V-s}$ . However these numbers are still far inferior when compared to their inorganic counterpart, which raises the question of whether doping with inorganic nanostructures such as ZnO would be beneficial. In the

blend, PCBM does not provide direct conduction pathways for electrons towards the electrode because of the isolated island formation. Electrons undergo a hopping process between PCBM islands before reaching the electrode. Thus, they become prone to recombination with holes. This limits the thickness of the active layer. High efficient P3HT:PCBM devices are achieved with active layer thickness around 100 nm to 200 nm, which is not the optimum thickness for photon absorption. Increasing the thickness absorbs more photons but it also increases the electron-hole recombination and degrades charge transport. The final stage of charge transport from point of exciton dissociation to the electrode is the crossing of the organic-inorganic interface. Large contact resistance will reduce the fill factor of a device. Potential barriers at the interface originating from impurities or polymer damage during vacuum deposition of the metal electrodes may also limit the open circuit voltage. Controlling the organic-inorganic interfacial properties is an important and urgent challenge in organic electronics. Several ways have already been explored such as insertion of very thin interlayer (Brabec et al., 2002), tuning the work function of the inorganic electrode (Sharma et al., 2009) and surface doping of polymer (Mukherjee et al., 2007).

#### 4.2 ZnO as electron acceptor

PCBM is the most widely used electron acceptor for P3HT in a bulk heterojunction (BHJ) solar cell. It has the right LUMO and HOMO levels for charge separation and exchange. Its electron mobility in the order of  $10^{-2}$  cm<sup>2</sup>/V-s, is sufficient for transporting photogenerated electrons towards the electrodes. However, higher mobilities are still demonstrated by inorganic materials. Wurtzite ZnO for example can have electron mobility of 200 cm<sup>2</sup>/V-s. Its LUMO and HOMO levels are well positioned to accept electrons from P3HT. Thus, doping of conjugated polymers with ZnO nanostructures can be employed to fabricate BHJ solar cells. For example, P3HT doped with ZnO nanoparticles yielded a photovoltaic device with  $\eta \sim 0.92\%$  at optimum concentration of 26% by volume (Beek et al., 2006). The values of the open circuit voltage ( $V_{OC}$ ), short circuit current density ( $J_{SC}$ ) and fill factor ( $FF$ ) were 0.69 V, 2.19 mA/cm<sup>2</sup> and 55% respectively. The authors employed the device structure: ITO/PEDOT:PSS/P3HT:ZnO/Al, which is a common structure used by P3HT:PCBM active layer. They identified the major performance limiting factors as the poor contact of P3HT with the ZnO and the coarse morphology. They also observed that thermal annealing of the active layer was very important.

In another work, ZnO nanofibers were grown on the transparent electrode to achieve fixed morphology before the introduction of the P3HT (Olson et al., 2007). By spin-coating the P3HT on top of the ZnO nanostructure followed by annealing, intercalation into the voids between the nanofibers was induced. In this structure, a huge donor-acceptor interface area is formed between the P3HT and ZnO for exciton dissociation. Photogenerated electrons injected into the ZnO are transported directly towards the collecting electrode, providing pathways with higher electron mobility. The growth of ZnO nanofibers on ITO-coated glass was achieved via a low-temperature hydrothermal route from a solution of zinc nitrate precursor. In this device structure in which Ag is used as back electrode instead of Al, electrons are collected by the ITO while holes are collected by the Ag. The best device they obtained had  $V_{OC}$ ,  $J_{SC}$  and  $FF$  of 0.44 V, 2.17 mA/cm<sup>2</sup> and 56% respectively corresponding to  $\eta \sim 0.53\%$ . Although this performance is relatively poorer than P3HT:PCBM devices ( $\eta \sim 5\%$ ), it is expected to improve when the major mechanisms in the device are better

understood. For example, the role of oxygen vacancies in the ZnO, which is the origin of visible emission, is not yet clear. Obtaining a balanced electron and hole mobilities in the active layer may also be a critical issue. Understanding the effect of ZnO on the effective Fermi level of the active layer, which determines the interfacial properties at the metal junction, is important. This may have a direct consequence on the  $V_{OC}$ . Lastly, the mechanism of aging in ambient air may give insights on how to optimize this device. The authors observed that right after fabrication, the device exhibited only little diode behavior. But after storing it in dark ambient air for 24 hours, better device performance was observed. In contrast, the device stored in dark argon environment decreased in performance. After 3 days in argon, the device performance continued to deteriorate whereas the performance of the device stored in air improved substantially. The improvement came from the increase in  $FF$  and  $V_{OC}$ . They explained this behavior in terms of the oxygen vacancies. These vacancies, which are intrinsic electron donors in ZnO, may be quenched when exposed to oxygen. As a result, semiconducting properties are improved as both the oxygen vacancy and carrier concentrations are reduced. This aging mechanism makes ZnO a very promising electron acceptor for BHJ solar cells, which require long term operation.

#### 4.3 Effect of ZnO nanowire doping on the Fermi level of P3HT

In polymer-based photovoltaics, it is important to obtain the desired junction characteristic of the polymer-metal interface. Depending on the device structure, it may require an Ohmic or a Schottky junction. The junction characteristic, which has a direct influence on the charge transfer from the active layer to the electrode, is determined by the energy level alignment of the polymer and the metal. Fermi level ( $E_F$ ) is the most fundamental parameter that is used to understand polymer-metal junction. It determines the work function (energy difference between  $E_F$  and vacuum level) of a material. It can be used to predict the built in potential ( $V_{bi}$ ) across a junction in thermal equilibrium. In thin film photovoltaic devices,  $V_{bi}$  is an essential parameter. It influences charge dissociation, charge transport and charge collection. Most importantly, it sets the maximum  $V_{oc}$  of a single junction solar cell. Thus, measurement of  $V_{bi}$  is very important practically and it can be a tool to understand how the  $E_F$  of a material behaves when it is doped. In most situations,  $V_{bi}$  across a junction is not equal to the value predicted by the difference in the  $E_F$  of each component. During the formation of the junction, such as the deposition of the metal on the polymer or the drying of the polymer on a metal surface, chemical reaction may occur. This leads to the existence of new compounds in the middle of the junction, which modifies the expected  $V_{bi}$ . Thus, determination of actual  $V_{bi}$  in real devices is more important practically because it takes into account the effect of processing. In photovoltaics for example, measuring  $V_{bi}$  in P3HT-Al junction formed by thermal evaporation of Al on P3HT film, is more meaningful than using a similar junction formed by spin-coating P3HT on Al film. This is because the first system is the one being used in the development of organic solar cells.

In this manuscript, recent results are presented about the change in the Fermi level of P3HT when doped with ZnO nanowires. This system is already being explored as an active layer together with Al as back electrode (Beek et al., 2006). To measure  $V_{bi}$ , capacitance-voltage (C-V) measurement was employed using an LCR meter. Test diodes were prepared by drop-casting P3HT and doped P3HT ( $\sim 1 \mu\text{m}$  thick) on Cr/Pt film then depositing Al on top via

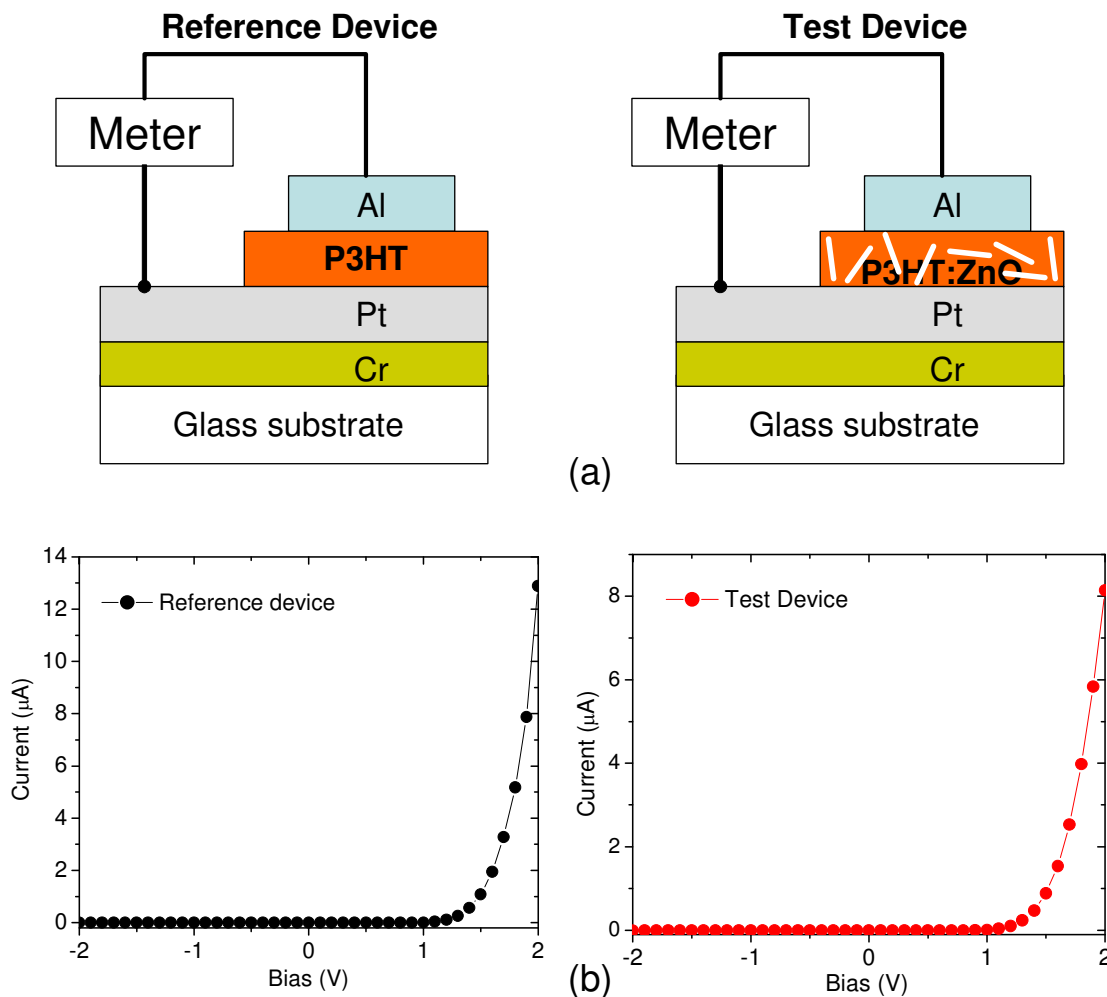


Fig. 5. (a) Device structure of the diodes used to measure the built in potential. (b)  $I$ - $V$  characteristic of the reference (pure P3HT) device and the test (ZnO-doped P3HT) device.

resistive thermal evaporation. The device structure is shown on Figure 5(a). Both doped and undoped devices exhibited good rectifying behaviour as depicted by their  $I$ - $V$  curves in Figure 5(b). The rectification is due to the Schottky junction formed by the polymer and Al. The high work function value of Pt ( $\sim 6.35$  eV) results in an Ohmic contact with the polymer. According to inorganic semiconductor theory, the capacitance  $C$  of the depletion layer is related to  $V_{bi}$  by the equation (Sze, 2007):

$$\frac{1}{C^2} = \frac{2(V_{bi} - V - kT/q)}{q\epsilon_s N_D} \quad (1)$$

Where  $V$  is the applied bias voltage,  $kT/q$  is the thermal voltage whose value at room temperature is 0.0259 V,  $\epsilon_s$  is the semiconductor permittivity and  $N_D$  is the donor impurity density.  $V_{bi}$  is determined by plotting this equation and finding the value of  $V$  where  $1/C^2$  extrapolates to zero. This is illustrated in Figure 6. The behavior of  $1/C^2$  is quite linear for both devices in the bias range of  $\pm 0.5$  V, consistent with equation (1). The solid line is the linear fit for each data set. Its intercept plus the thermal voltage is equal to  $V_{bi}$ . The obtained value for the pure P3HT is 1.243 V. This is fairly close to the expected value based on the  $E_L$

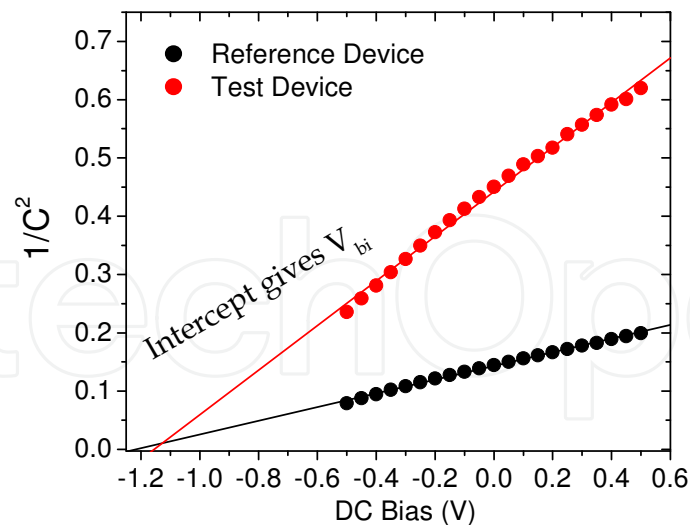


Fig. 6. Plot of  $1/C^2$  where  $C$  is the depletion layer capacitance as a function of applied DC bias. The intercept of the linear fit gives the built in potential.

offset between P3HT and Al. The work function of P3HT is around 5.1 to 5.2 eV. For Al, it ranges from 4.0 to 4.3 eV. The ZnO-doped P3HT has  $V_{bi}$  of 1.181V, indicating that  $E_F$  of the P3HT moved farther from the valence band edge and closer to the  $E_F$  of Al. One possible explanation for this reduction is the increase in the free electron concentration in the polymer nanocomposite provided by the ZnO. In semiconductors,  $E_F$  lies closer to the conduction band edge for  $n$ -type conductivity and it lies closer to the valence band edge for  $p$ -type conductivity. The upward shift in  $E_F$  due to the ZnO may be the cause of the drop in  $V_{OC}$  for P3HT:ZnO nanofibers BHJ (Olson et al., 2007). When the authors compared the photovoltaic performance of ZnO bilayer and ZnO nanofiber devices, they observed higher  $V_{OC}$  in the bilayer device (500 mV versus 440 mV). Although the nanofiber device still had better  $\eta$  due to its higher  $J_{SC}$ . The results shown in Figure 6 may be helpful in optimizing BHJ solar cell based on P3HT and ZnO nanostructures. High values of  $J_{SC}$  and  $V_{OC}$  may be obtained simultaneously by tailoring the property of the active layer-metal interface or selecting alternative metals or alloys for back electrode.

## 5. Polymer-based conductivity sensors

### 5.1 Conductivity sensors for chemical detection

Conductivity sensors for chemical detection are very attractive because of their simple operation. The circuit design required to convert their response to electrical signals is relatively straightforward. These sensors are based on the change in the electrical conductivity of the sensing material due to its interaction with the stimuli. Device fabrication is also not difficult. For example, the sensing material may be deposited on interdigitated or two parallel electrodes, which form the connection for measuring the change in electrical resistance. Three common classes of sensing materials for conductivity sensors are conducting polymer composites, intrinsically conducting polymers and metal oxides (Arshak et al., 2004). The mechanism behind the change in conductivity is different for each class.

In conducting polymer composites, conducting particles such as polypyrrole and carbon black (Albert et al., 2000) are embedded in an insulating polymer matrix. The stimuli can cause expansion of the polymer and the polypyrrole particles resulting in the increase of electrical resistance. If the stimuli interact chemically with the polypyrrole, its intrinsic conductivity will also change, making the resistance change in the composite more difficult to interpret. The operation of intrinsically conducting polymers (ICP) such as polypyrrole, polythiophene and polyaniline, is based on the alteration of intrachain conductivity, intermolecular conductivity and ionic conductivity after interacting with the stimuli. Intrachain conductivity is determined by the backbone while intermolecular conductivity is due to electron hopping to different chains. Ionic conductivity is affected by proton tunneling induced by hydrogen bond interaction at the backbone and also by ion migration through the polymer. One reported application of ICP employed an array of conducting polymer sensors incorporating 3-Methylthiophene, Aniline and Pyrrole (Guadarrama et al., 2000). The authors evaluated the sensors to different wine varieties and considered the cross sensitivity of the polymeric films to moisture and ethanol. The operation of a metal oxide sensor is based on the dependence of the conductivity to  $O_2$  molecules adsorbed on its surface. For *n*-type metal oxides such as ZnO or  $TiO_2$ ,  $O_2$  molecules capture electrons on the surface or at the grain boundaries resulting in the decrease of conductivity. Trapped electrons at the grain boundaries also produce potential barriers between grains that impede current flow. When exposed to reducing gas like  $H_2$ ,  $CH_4$ , CO,  $C_2H_5$  or  $H_2S$ , the adsorbed  $O_2$  molecules react with the gas and release the captured electrons. This increases the conductivity of the sensing material. When exposed to oxidizing gas like  $O_2$ ,  $NO_2$  or  $Cl_2$ , the effect is opposite. Conductivity is decreased because the number of adsorbed  $O_2$  molecules that can capture electrons is increased. For *p*-type metal oxides, their response to oxidizing gas is to increase in conductivity because the capture of electrons produces more holes. In contrast, their conductivity decreases when exposed to reducing gases.

There are still many challenges in conductivity gas sensors. For polymer composites, aging is a concern because this leads to sensor drift. Their applicability is only limited to certain gases because of lack of sensitivity. For ICP, challenges include understanding the mechanism of sensor response, high sensitivity to humidity and drift in conductivity with time. These sensors can also have short lifetimes due to oxidation of the polymer. For metal oxides, one challenge is the low sensitivity at room temperature. They require higher operating temperatures and thus heating element has to be incorporated with the sensor (Roy & Basu, 2002) This increases the power consumption, which is not very appealing for handheld applications. Good selectivity is another challenge for metal oxide conductivity sensors. Their behavior to reducing gases is practically the same. For example, the conductivity of a sensor changed by  $\Delta$  when exposed to ethanol vapor with concentration  $C_1$ . The same response can be realized when it is exposed to methanol with a different concentration  $C_2$ . Thus, the identification of a particular reducing vapor, with a background of different others is almost impossible. Due to the mentioned challenges, there is a continuous effort to develop new materials for conductivity sensors. Reliable sensors with appropriate levels of selectivity and sensitivity will always be in demand. In the standpoint of defense and homeland security, new hazardous compounds or biomaterials that need to be detected is expected to arise. New applications such as self-powered sensors will require excellent energy efficient sensing materials without sacrificing sensitivity and selectivity.

### 5.2 Sensing with P3HT doped with ZnO nanowires

There is a lack of work in the exploration of ZnO doped polymers as conductivity sensors for chemical detection. Interestingly, only P3HT, which is mostly used in photovoltaics, has been reported to have promising sensing behavior when blended with ZnO-NWs (Saxena et al., 2007). As separate materials, P3HT and ZnO-NWs can both be used as a conductivity gas sensor. But due to the difference in their conductivity type, they have contrasting response to a specific stimulus. For example, they both exhibit high sensitivity to NO<sub>2</sub> and H<sub>2</sub>S (Saxena et al., 2007). P3HT decreases in resistance upon exposure to NO<sub>2</sub>, which is oxidizing gas, while it behaves oppositely for H<sub>2</sub>S, a reducing gas. This characteristic is due to its *p* - type conductivity. The adsorption of an oxidizing compound on P3HT surface captures electrons leading to increased hole carrier concentration. Conversely, the adsorption of a reducing compound leads to the decrease in hole carrier concentration via the release of captured electrons. For *n* - type ZnO, the effect of oxidizing and reducing compounds is to decrease and increase conductivity respectively.

Doping of P3HT with oxygen deficient ZnO nanowires results in the reduction of P3HT. This is well supported by GI-XRD, XPS and FTIR studies (Saxena et al., 2007). The authors also observed decrease in the P3HT conductivity after ZnO doping suggesting that its hole carrier concentration drops when ZnO donates electrons. This interaction may be used to tailor the response of polymers to different stimuli, opening up the possibility of tunable polymer-based conductivity sensors. For example, the authors have demonstrated that highly reduced P3HT resulting from ZnO doping, has enhanced sensitivity to NO<sub>2</sub> because this chemical can easily pick up electrons from P3HT to get adsorbed as NO<sub>2</sub><sup>-</sup> ions. They have obtained room temperature sensors that can detect NO<sub>2</sub> in the 0 - 10 ppm range with very high selectivity. In contrast, the sensitivity of ZnO-doped P3HT to a reducing H<sub>2</sub>S is weakened because it is difficult to further reduce the P3HT.

## 6. Conclusion

As separate materials, polymers and ZnO are already considered to be important technologically. They have found several commercial applications in optoelectronics and sensors. Despite that, research activities involving these materials are still in full swing. For example, there is a lot of effort in developing high efficient polymeric solar cells and light emitting diodes. One of the big challenges in this area is long term stability. For ZnO, most of its expected applications, such as UV light emitters, spin functional devices, chemical sensors, surface acoustic wave devices and transparent conductors, are still in the laboratory level. This is mainly because ZnO is prone to material defects that it becomes very difficult to obtain reproducible device performance and reliability. Clearly, there is still a considerable work to be done with ZnO alone, but it is worthwhile to broaden its potential as a technological material. In this manuscript, a more unique role of ZnO, which is as a dopant to polymers, has been presented. This is an area of research, which is just beginning to be explored. Relevant publications are still limited but they report some intriguing observations that may have novel optoelectronic and sensor applications. The interaction of ZnO with polymers may provide ways of obtaining unique or enhanced optical and electronic properties in polymer nanocomposites. Thus, by doping polymers with ZnO, new applications may be realized without losing the benefits offered by polymers in terms of processing, scalability and mechanical flexibility.

## 7. References

- Albert, K.; Lewis, N.; Schauer, C.; Sotzing, G.; Stitzel, S.; Vaid, T. & Walt, D. (2000). Cross-reactive chemical sensor arrays. *Chemical Reviews*, Vol. 100, No. 7, (June 2000) 2595 – 2626, ISSN 1520-6890
- Aleshin, A.; Shcherbakov, I.; Alexandrova, E. & Lebedev, E. (2008). Effect of electric field on the photoluminescence of polymer-inorganic nanoparticle composites. *Solid State Communications*, Vol. 146, No. 3-4, (April 2008) 161 – 165, ISSN 0038-1098
- Aleshin, A.; Alexandrova, E. & Shcherbakov, I. (2009). Hybrid active layers from a conjugated polymer and inorganic nanoparticles for organic light emitting devices with emission colour tuned by electric field. *Journal of Physics D: Applied Physics*, Vol. 42, No. 10, (May 2009) 105108, ISSN 1361-6463
- Arshak, K.; Moore, E.; Lyons, G.; Harris, F. & Clifford, S. (2004). A review of gas sensors employed in electronic nose applications. *Sensor Review*, Vol. 24, No. 2, (April 2004) 181 – 198, ISSN 0260-2288
- Beek, W.; Wienk, M. & Janssen, R. (2006). Hybrid solar cells from regioregular polythiophene and ZnO nanoparticles. *Advanced Functional Materials*, Vol. 16, No. 8, (May 2006) 1112-1116, ISSN 1616-3028
- Bennett, G.; Greenbaum, S. & Owens, F. (2009). NMR and Raman spectroscopic characterization of single walled carbon nanotube composites of polybutadiene. *Journal of Material Research*, Vol. 24, No. 7, (July 2009) 2215 - 2220, ISSN 0884-2914
- Blom, P.; de Jong, M. & van Munster, M. (1997). Electric-field and temperature dependence of the hole mobility in poly(*p* - phenylene vinylene). *Physical Review B*, Vol. 55, No. 2, (January 1997) 656 – 659, ISSN 1538-4489
- Brabec, C.; Shaheen, S.; Winder, C. & Sariciftci, N. (2002). Effect of LiF/metal electrodes on the performance of plastic solar cells. *Applied Physics Letters*, Vol. 80, No. 7, (February 2002) 1288-1290, ISSN 1077-3118
- Cheng, B.; Shi, W.; Russell-Tanner, J.; Zhang, L. & Samulski, E. (2006). Synthesis of variable-aspect-ratio, single-crystalline ZnO nanostructures. *Inorganic Chemistry*, Vol. 45, No. 3, (January 2006) 1208 – 1214, ISSN 0020-1669
- Chiang, C.; Druy, M.; Gau, S.; Heeger, A.; Louis, E. ; MacDiarmid, A. & Shirakawa, H. (1978). Synthesis of highly conducting films of derivatives of polyacetylene, (CH)<sub>x</sub>. *Journal of the American Chemical Society*, Vol. 100, No. 3, (February 1978) 1013 - 1015, ISSN 1520-5126
- Chirvase, D.; Parisi, J.; Hummelen, J. & Dyakonov, V. (2004). Influence of nanomorphology on the photovoltaic action of polymer-fullerene composites. *Nanotechnology*, Vol. 15, No. 9, (August 2004) 1317-1323, ISSN 1361-6528
- Dijken, A.; Meulenkaamp, E.; Vanmaekelbergh, D. & Meijerink, A. (2000). The kinetics of the radiative and nonradiative processes in nanocrystalline ZnO particles upon photoexcitation. *Journal of Physical Chemistry B*, Vol. 104, No. 8, (February 2000) 1715 – 1723, ISSN 1520-6106
- Guadarrama, A.; Fernandez, J.; Iniguez, M.; Souto, J. & de Saja, J. (2000). Array of conducting polymer sensors for the characterisation of wines. *Analytica Chimica Acta*, Vol. 411, No. 1-2, (May 2000) 193 – 200, ISSN 0003-2670

- Huang, M.; Mao, S.; Feick, H.; Yan, H.; Wu, Y.; Kind, H.; Weber, E.; Russo, R. & Yang, P. (2001). Room-temperature ultraviolet nanowire nanolasers. *Science*, Vol. 292, No. 5523, (June 2001) 1897 - 1899, ISSN 1095-9203
- Kim, J.; Ingrosso, C.; Fakhfour, V.; Striccoli, M.; Agostiano, A.; Curri, M. & Brugger, J. (2009). Inkjet-printed multicolor arrays of highly luminescent nanocrystal-based nanocomposites. *Small*, Vol. 5, No. 9, (February 2009) 1051 - 1057, ISSN 1613-6829
- Kim, D.; Yang, J. & Hong, J. (2009). Ferromagnetism induced by Zn vacancy defect and lattice distortion in ZnO. *Journal of Applied Physics*, Vol. 106, No. 1, (July 2009) 013908, ISSN 1089-7550
- Koji, N.; Tomonori, Y.; Kenji, I. & Fumio, S. (1999). Properties and structure of poly(vinyl alcohol)/silica composites. *Journal of Applied Polymer Science*, Vol. 74, No. 1, (October 1999) 133 - 138, ISSN 1097-4628
- Konenkamp, R.; Word, R. & Schlegel, C. (2004). Vertical nanowire light emitting-diode. *Applied Physics Letters*, Vol. 85, No. 24, (December 2004) 6004 - 6006, ISSN 1077-3118
- Koster, L.; Mihailetschi, V. & Blom, P. (2006). Ultimate efficiency of polymer/fullerene bulk heterojunction solar cells. *Applied Physics Letters*, Vol. 88, No. 9, (March 2006) 093511, ISSN 1077-3118
- Li, Z.; Xiong, Y. & Xie, Y. (2003). Selected-control synthesis of ZnO nanowires and nanorods via a PEG-assisted route. *Inorganic Chemistry*, Vol. 42, No. 24, (October 2003) 8105 - 8109, ISSN 0020-1669
- Liu, B. & Zeng, C. (2004). Room temperature solution synthesis of monodispersed single-crystalline ZnO nanorods and derived hierarchical nanostructures. *Langmuir*, Vol. 20, No. 10, (April 2004) 4196 - 4204, ISSN 0743-7463
- Ma, W.; Yang, C.; Gong, X.; Lee, K. & Heeger, A. (2005). Thermally stable, efficient polymer solar cells with nanoscale control of the interpenetrating network. *Advanced Functional Materials*, Vol. 15, No. 10, (October 2005) 1617-1622, ISSN 1616-3028
- Meulenkamp, E. (1998). Synthesis and Growth of ZnO nanoparticles. *Journal of Physical Chemistry B*, Vol. 102, No. 29, (June 1998) 5566 - 5572, ISSN 1520-6106
- Morteani, A.; Ho, P.; Friend, R.; & Silva, C. (2005). Electric field-induced transition from heterojunction to bulk charge recombination in bilayer polymer light-emitting diodes. *Applied Physics Letters*, Vol. 86, No. 16, (May 2005) 163501, ISSN 1077-3118
- Mukherjee, A.; Thakur, A.; Takashima, W. & Kaneto, K. (2007). Minimization of contact resistance between metal and polymer by surface doping. *Journal of Physics D: Applied Physics*, Vol. 40, No. 6, (March 2007) 1789-1793, ISSN 1361-6463
- Musikhin, S.; Bakueva, L.; Sargent, E. & Shik, A. (2002). Luminescent properties and electronic structure of conjugated polymer-dielectric nanocrystal composites. *Journal of Applied Physics*, Vol. 91, No. 10, (May 2002) 6679-6683, ISSN 1089-7550
- Norton, D.; Heo, Y.; Ivill, M.; Ip, K.; Pearton, S.; Chisholm, M. & Steiner, T. (2004). ZnO: growth, doping & processing. *Materials Today*, Vol. 7, No. 6, (June 2004) 34 - 40, ISSN 1369-7021
- Olson, D.; Shaheen, S.; Collins, R. & Ginley, D. (2007). The effect of atmosphere and ZnO morphology on the performance of hybrid poly(3-hexylthiophene)/ZnO nanofiber

- photovoltaic devices. *Journal of Physical Chemistry C*, Vol. 111, No. 44, (October 2007) 16670 – 16678, ISSN 1932-7455
- Roy, S. & Basu, S. (2002). Improved zinc oxide film for gas sensor applications. *Bulletin of Material Science*, Vol. 25, No. 6, (November 2002) 513 – 516, ISSN 0250-4707
- Saxena, V.; Aswal, D.; Kaur, M.; Koiry, S.; Gupta, S.; Yakhmi, J.; Kshirsagar, R. & Deshpande, S. (2007). Enhanced NO<sub>2</sub> selectivity of hybrid poly(3-hexylthiophene): ZnO-nanowire thin films. *Applied Physics Letters*, Vol. 90, No. 4, (February 2007) 043516, ISSN 1077-3118
- Shalish, I.; Temkin, H. & Narayanamurti, V. (2004). Size-dependent surface luminescence in ZnO nanowires. *Physical Review B*, Vol. 69, No. 24, (June 2004) 245401, ISSN 1538-4489
- Shan, W.; Walukiewicz, W.; Ager III, J.; Yu, K.; Yuan, H.; Xin, H.; Cantwell, G. & Song, J. (2005). Nature of room-temperature photoluminescence in ZnO. *Applied Physics Letters*, Vol. 86, No. 19, (May 2005) 191911, ISSN 1077-3118
- Sharma, A.; Hotchkiss, P.; Marder, S. & Kippelen, B. (2009). Tailoring the work function of indium tin oxide electrodes in electrophosphorescent organic light-emitting diodes. *Journal of Applied Physics*, Vol. 105, No. 8, (April 2009) 084507, ISSN 1089-7550
- Sui, X.; Shao, C. & Liu, Y. (2005). White-light emission of polyvinyl alcohol/ZnO hybrid nanofibers prepared by electrospinning. *Applied Physics Letters*, Vol. 87, No. 11, (September 2005) 113115, ISSN 1077-3118
- Sun, D.; Sue, H-J. & Miyatake, N. (2008). Optical properties of ZnO quantum dots in epoxy with controlled dispersion. *Journal of Physical Chemistry C*, Vol. 112, No. 41, (September 2008) 16002 – 16010, ISSN 1932-7455
- Sze, S. (2007). *Physics of Semiconductor Devices*, John Wiley & Sons, Inc. ISBN-13: 978-0-471-14323-9, Hoboken NJ USA
- Ton-That, C.; Phillips, M. & Nguyen, T-P. (2008). Blue shift in the luminescence spectra of MEH-PPV films containing ZnO nanoparticles. *Journal of Luminescence*, Vol. 128, No. 12, (July 2008) 2031 - 2034, ISSN
- Ton-That, C.; Phillips, M.; Foley, M.; Moody, S. & Stampfl, A. (2008). Surface electronic properties of ZnO nanoparticles. *Applied Physics Letters*, Vol. 92, No. 26, (July 2008) 261916, ISSN 1077-3118
- Umeda, J.; Sakamoto, W. & Yogo, T. (2009). Synthesis and field-responsive properties of SrTiO<sub>3</sub> nanoparticle/polymer hybrid. *Journal of Material Research*, Vol. 24, No. 7, (July 2009) 2221 - 2228, ISSN 0884-2914
- Wang, Q.; Pflugl, C.; Andress, W.; Ham, D. & Capasso, F. (2008). Gigahertz surface acoustic wave generation on ZnO thin films deposited by radio frequency magnetron sputtering on III-V semiconductor substrates. *Journal of Vacuum Science Technology B*, Vol. 26, No. 6, (November 2008) 1848 - 1851, ISSN 1520-8567
- Winey, K. & Vaia, R. (2007). Polymer nanocomposites. *MRS Bulletin*, Vol. 32, No. 4, (April 2007) 314 - 322, ISSN 0883-7694
- Xu, Z-X.; Roy, V.; Stallinga, P.; Muccini, M.; Toffanin, S.; Xiang, H-F. & Che, C-M. (2007). Nanocomposite field effect transistors based on zinc oxide/polymer blends. *Applied Physics Letters*, Vol. 90, No. 22, (June 2007) 223509, ISSN 1077-3118

Zhang, T.; Xu, Z.; Qian, L.; Tao, D.; Teng, F. & Xu, X. (2006). Influence of ZnO nanorod on the luminescent and electrical properties of fluorescent dye-doped polymer nanocomposite. *Optical Materials*, Vol. 29, No. 2, (November 2006) 216 - 219, ISSN 0925-3467

IntechOpen

IntechOpen



## **Nanowires Science and Technology**

Edited by Nicoleta Lupu

ISBN 978-953-7619-89-3

Hard cover, 402 pages

**Publisher** InTech

**Published online** 01, February, 2010

**Published in print edition** February, 2010

This book describes nanowires fabrication and their potential applications, both as standing alone or complementing carbon nanotubes and polymers. Understanding the design and working principles of nanowires described here, requires a multidisciplinary background of physics, chemistry, materials science, electrical and optoelectronics engineering, bioengineering, etc. This book is organized in eighteen chapters. In the first chapters, some considerations concerning the preparation of metallic and semiconductor nanowires are presented. Then, combinations of nanowires and carbon nanotubes are described and their properties connected with possible applications. After that, some polymer nanowires single or complementing metallic nanowires are reported. A new family of nanowires, the photoferroelectric ones, is presented in connection with their possible applications in non-volatile memory devices. Finally, some applications of nanowires in Magnetic Resonance Imaging, photoluminescence, light sensing and field-effect transistors are described. The book offers new insights, solutions and ideas for the design of efficient nanowires and applications. While not pretending to be comprehensive, its wide coverage might be appropriate not only for researchers but also for experienced technical professionals.

### **How to reference**

In order to correctly reference this scholarly work, feel free to copy and paste the following:

Aga and Mu (2010). Doping of Polymers with ZnO Nanostructures for Optoelectronic and Sensor Applications, Nanowires Science and Technology, Nicoleta Lupu (Ed.), ISBN: 978-953-7619-89-3, InTech, Available from: <http://www.intechopen.com/books/nanowires-science-and-technology/doping-of-polymers-with-zno-nanostructures-for-optoelectronic-and-sensor-applications>

**INTECH**  
open science | open minds

### **InTech Europe**

University Campus STeP Ri  
Slavka Krautzeka 83/A  
51000 Rijeka, Croatia  
Phone: +385 (51) 770 447  
Fax: +385 (51) 686 166  
[www.intechopen.com](http://www.intechopen.com)

### **InTech China**

Unit 405, Office Block, Hotel Equatorial Shanghai  
No.65, Yan An Road (West), Shanghai, 200040, China  
中国上海市延安西路65号上海国际贵都大饭店办公楼405单元  
Phone: +86-21-62489820  
Fax: +86-21-62489821

© 2010 The Author(s). Licensee IntechOpen. This chapter is distributed under the terms of the [Creative Commons Attribution-NonCommercial-ShareAlike-3.0 License](#), which permits use, distribution and reproduction for non-commercial purposes, provided the original is properly cited and derivative works building on this content are distributed under the same license.

IntechOpen

IntechOpen